Towards Automatic Detection of Dark Features in the Barents Sea using Synthetic Aperture Radar

Anca Cristea, A. Malin Johansson, *Member, IEEE,* Natalya A. Filimonova, Dmitry V. Ivonin, Nicholas Hughes, *Member, IEEE,* Anthony P. Doulgeris, *Member, IEEE,* and Camilla Brekke, *Member, IEEE,*

***Abstract*—Increased human presence and commercial activities in the Barents Sea (fishing, offshore oil and gas exploration) are amplifying the need for large-scale operational ocean monitoring of the eventual oil spills in the region. The geographical location and climate impose additional constraints on satellite-based monitoring, making it necessary to use Synthetic Aperture Radar (SAR). Dark features or low backscatter areas are frequent within the SAR images and their occurrence may indicate oil spills or so-called lookalikes. Automatic oil spill detection hinges on accurate separation of the *lookalikes* from actual oil spills. Two main types exist in the Barents Sea: newly formed sea ice and low wind regions, where the former occur during the freezing part of the year (approx. November - April) and the other year around. Mapping the occurrence of oil spills and lookalikes in the Barents Sea on a seasonal basis would add to our understanding and knowledge of the low backscatter phenomena. Awareness of the major locations of oil spills, natural oil seeps, or lookalikes, are important for operational services and their effort to reduce false alarms. Here, we explore the use of a segmentation-based dark feature detection method with Sentinel-1 Extra Wide-Swath SAR images. We test the method on images acquired over the Barents Sea during the freezing season, and cross-validate the results with two sets of dark features segmented by operational expert oil spill and sea ice monitoring services. The results are discussed, together with currently developing method improvements, all while working towards a fully-automated method for monitoring dark features in the Barents Sea.**

***Index Terms*—Oil slicks, newly formed sea ice, SAR, polarimetry, Arctic**

I. Introduction

DARK features in Synthetic Aperture Radar (SAR) constitute signatures of low backscatter areas of various shapes, extents and origins. Within the Arctic ocean, a common dark feature is represented by the thinnest ice types including new ice, nilas, and young ice [1], but also e.g., oil slicks (mineral or animal) and low wind regions. Oil slicks are more common along the commercial shipping routes or in the vicinity of oil and gas platforms in the Barents Sea [2], whereas new ice formation takes place in, e.g., the marginal ice zone (MIZ) and leads [3]. Newly formed sea ice and leads provide safe routing for ship traffic and cost-effective passage through the sea ice, therefore oil slicks may occur in their vicinity. Advanced Microwave Scanning Radiometer 2 (AMSR2) data was used to identify the peak in new ice formation for the Barents and Kara Seas as occurring between October and February, though with large inter-annual variations [3]. In the context of operational monitoring, using the finer resolution SAR could enhance the detection of dark features with potentially small dimensions and irregular shapes.

SAR satellite images have a long history of being used for operational surveillance of ocean areas, detection of marine oil slicks and classification of sea ice types. This is possible thanks to the nature of radar imaging, which is independent of natural light or cloud cover. The spatial coverage and the temporal resolution (twice daily coverage of the Extra Wide (EW) mode in the HH/HV configuration over the Arctic Ocean) offered by Sentinel-1 as well as the free data policy makes it the obvious SAR data source. This paper presents an automatic method for the detection of dark features in Sentinel-1 EW imagery. The method consists in selecting segments with low backscatter produced by a segmentation algorithm based on statistical mixtures [4] [5].

In the EW mode, data is acquired under a range of incidence angles spanning over approx. 28^o, which implies considerable intensity decay from near to far range [6] [7]. The segmentation algorithm merges theoretical aspects and empirical observations into a statistical model that accounts for the decay by assuming non-stationary per-segment means [5]. This ensures that the dark features are encapsulated within the same segments. In order to demonstrate the performance of our method, we have selected two Sentinel-1 EW images acquired in the Barents Sea and containing dark features that extend throughout the range. The automatically segmented dark features are also compared with a set of manually segmented dark features provided by operational oil spill detection services at ScanEx Moscow, as well as with sea ice classifications with specific emphasis on new ice types carried out by experts at the Norwegian Ice Service.

The main purpose of this study is to demonstrate the ability of the proposed method to identify dark features. The long term objective is to work towards identifying the locations and times of the year where dark features are most pronounced. In order to accomplish this, a thorough assessment of a larger dataset will be required and constitutes ongoing work.

II. Method

Our proposed dark feature detection method is automatic and consists of a segmentation step and a dark feature selection step.

A. Cristea, A. M. Johansson, A. P. Doulgeris and C. Brekke are with the Department of Physics and Technology, UiT The Arctic University of Norway, 9037 Tromsø, Norway. N. A. Filimonova is with the SCANEX Group, Operational monitoring department, Moscow, Russia. D. V. Ivonin is with Shirshov Institute of Oceanology RAS, Moscow, Russia. N. Hughes is with the Norwegian Meteorological Institute (MET), Tromsø, Norway.

A. Segmentation

SAR image segmentation is performed using the statistical mixture model-based algorithm presented in [4] and [5]. Each mixture component is meant to model the natural variability in backscattering coefficients [dB] (equivalent to log-intensities) measured for a physical structure with relatively homogeneous scattering properties (for example open water affected by wind of a certain speed, an oil film, a type of sea ice with uniform roughness etc.). The end segments are produced by splitting the mixture into these components. The model is a Gaussian mixture modified to allow varying means for the components, in order to account for incidence angle effects that manifest as approximately linear backscattering coefficient decays from near to far range. Moreover, the decay rates are free to vary between components, as structures with different scattering properties are known to present not only different degrees of backscatter variability at a specific range, but also different backscatter decay rates with incidence angle ([8], [6]). The segmentation is essentially performed by separating the mixture components using an iterative Expectation-Maximization scheme, which converges when all the estimated components are fitted by the model to a specific level set by a goodness-of-fit test. The end result consists in a variable number of segments, depending on the subset of samples selected for the estimation procedure. In the two examples presented here, approximately 0.5 % of the total image samples were used to determine the segments.

Prior to segmentation, the input intensities are calibrated to Sigma Nought, and the original product land masks are used to exclude the land pixels from the analysis. The algorithm is designed for multi-channel use, but is here employed on single-channel intensities for two reasons. Firstly, as the sought-after dark features produce evident signatures in the co-polarized (HH) channel due to very low scattering from the surface, they can usually be detected by using this channel alone. Secondly, the cross-polarized (HV) channel in the Sentinel-1 EW mode is often severely affected by noise, which in turn can have a negative impact on the segmentation result.

B. Dark feature selection

In addition to segments, the algorithm outputs segment features, of which the mean intensity [dB] at $\theta = 0^\circ$ and the decay rate [dB/$^\circ$] are of interest here for segment selection. At this stage, the segment with the lowest intensity at incidence angle $\theta = 32^\circ$ is simply selected as the dark feature. The value of 32° is chosen to be approximately mid-range in order to ensure consistency between images. As the dark features are defined as having backscatter values lower than their surroundings (below -20 dB at $\theta = 32^\circ$), it is often the case that the chosen segment maintains the lowest intensity throughout the range.

The post-extraction results were then compared to the two validation datasets provided by ScanEx Moscow and the Norwegian Ice service, both of which are presented in Section IV. The segments were overlayed for visual interpretation. Moreover, the overlap between the automatically and manually obtained segments has been computed as an initial validation measure.

III. SAR DATA

We use medium-resolution Sentinel-1 EW images covering parts of the Barents Sea. The images have a 100 m x 100 m resolution, a swath width of 410 km and an incidence angle range of 18.9–47.0 ^{o}. The selected images were taken during the freezing season, when the mean temperature is expected to be below -5^{o}C [3]. Image #1 (Fig. 1(a)) was acquired on November 29 2017 at 03:00 UTC and image #2 (Fig. 1(c)) on March 25 2019 at 03:39 UTC, and both were acquired in descending pass. The two images were chosen as they contain dark features throughout most of the range, including both newly formed sea ice and low wind regions, and in both images ScanEx Moscow confirmed the absence of oil slicks and presence of ice. Only the co-polarized channel (HH) was used for detection.

IV. VALIDATION DATA

In order to assess and validate the automatically obtained segments, we used two complementary datasets obtained via two different methods applied to the dark feature areas from the test images.

The first dataset contains segments identified manually by the operational oil slick detection service of ScanEx Moscow. The identification was based on visual examination of the images, after the absence of oil was confirmed using the semi-automatic approach of [2]. The dark feature areas were clearly identified and delineated down to pixel resolution, thereby enabling a quantitative pixel-to-pixel comparison with the results from the automatic detection algorithm.

For the second validation dataset, sea ice experts at the Norwegian Ice Service identified the newly formed sea ice areas using the same two Sentinel-1 images, but also complemented them with Copernicus Marine Environment Monitoring Service (CMEMS) sea surface temperature (SST) data. Inclusion of SST data enables separation of areas with temperatures above freezing ($>$-1.8^{o}C) from those below freezing. This is important, as ocean areas with too high temperatures are unlikely to contain newly formed sea ice, though could possibly contain oil slicks or be affected by low winds. In this validation dataset, larger polygons cover broad regions containing newly formed sea ice with both low and high backscatter, therefore only a qualitative comparison is possible.

V. PRELIMINARY RESULTS AND DISCUSSION

Fig. 1 shows the two original Sentinel-1 scenes (a and c), as well as the dark features identified by our method and overlapping validation data (b and d).

Scene #1 contains newly formed sea ice with varying levels of brightness, as the smooth regions show up as dark, while the more rough, fragmented regions as slightly brighter. The automatically identified segments contain only the darkest regions, while the manually delineated segments from dataset 1 also incorporate the brighter parts considered by the experts as part of the dark feature. Therefore, some differences stem

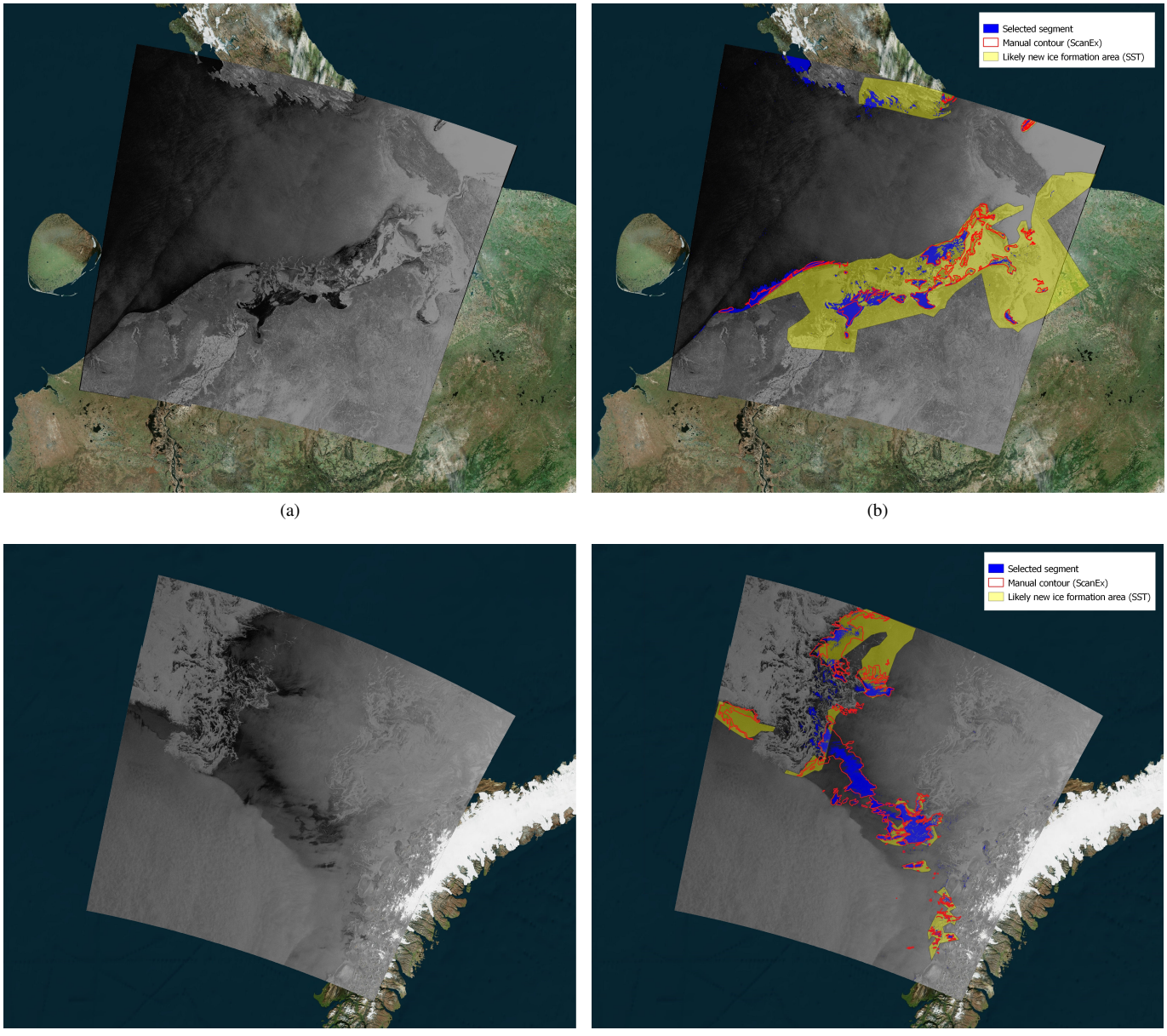

Fig. 1. The two Sentinel-1 EW images (HH Intensities in dB) and identified dark features. The left column shows the Sentinel-1 images #1 (a) and #2 (c) and the right column (#1 (b) and #2 (d)) shows the identified dark features. Automatically identified dark feature segments are shown in blue, validation dataset 1 is represented by red outlines and validation dataset 2 by the bright yellow areas.

from the slightly different definitions of the dark features, and may be eliminated by adding a segment fusion step. The visual expert opinion is furthermore supported by the sea ice validation dataset (dataset 2), which outlines the likely new ice formation region. The automatic segments are also covered by dataset 2, with the exception of a few dark areas on the southern tip of Novaya Zemlya. The discrepancy highlights the importance of secondary analysis of the automatically obtained segments, which may include a manual step for the removal of some areas. As an alternative, it is worth exploring the use of complementary information from the cross-polarized channel for the exclusion of areas that may be incorrectly included in the dark feature segment.

Scene #2 is more complex due to the presence of low backscatter regions representing both freezeup areas and low wind areas. The latter can be seen in the central part of the scene, and was confirmed by SST data used in dataset 2, where the temperatures were too high to support new ice formation. In the western extremity of the scene, we can observe a dark feature that was not detected by the segmentation algorithm. This is likely due to the positioning of the feature in the far range, where intensity values are approaching the noise floor and the reliability of the segments decreases. Additional differences between the automatically and manually determined segments are, as in the first scene, determined by variations in backscatter intensities within the dark features.

A quantitative comparison was performed between the au-

tomatically and manually obtained segments by considering the latter as reference. The automatically detected segments were found to overlap with 56 % of the reference for scene 1, respectively 48 % for scene 2. Additional steps will be required for a more precise detection. However, considering that the contours of the dark areas are very well determined, even a semi-automatic approach would be superior to a full-on manual approach.

VI. Conclusions and future work

The proposed method is able to identify dark features across an entire wide-swath SAR image, thereby ensuring that dark features covering different incidence angles are combined into one coherent segment within each image. The qualitative comparison with manually selected dark features shows that the overlap is generally good and the segment outlines are well determined. The discrepancies observed in both the qualitative and quantitative analysis may be diminished by adding a manual step to the method, or by exploring algorithm improvements. One such improvement is currently being developed and consists in the integration of a variable noise-floor model for the mean of the intensity distribution, in order to reduce errors originating from noise artefacts. This will also allow the use of the cross-polarized channel as complementary data. Moreover, segment selection was performed here in a very simplistic way, and segment fusion could be a better option if the dark features are defined as including variable intensity levels. Lastly, our analysis suggests that the integration of, e.g., CMEMS SST products into the method may ensure the separation of low wind areas from the other dark features.

Acknowledgment

This research is financed by CIRFA (RCN Grant no. 237906), OIBSAR (RCN Grant no. 280616), and the Russian Foundation for Basic Research under grants No.18-55-20010. The Sentinel-1 data was provided through Copernicus and processed by ESA.

References

[1] Secretary of the World Meteorological Organisation, *WMO Sea-Ice Nomenclature: Terminology, Codes and Illustrated Glossary*, rev. march 2014 ed. Geneva, Switzerland: World Meteorological Organisation, 1970, vol. 259.

[2] A. Ivanov, N. Filimonova, A. Kucheiko, N. Evtushenko, and N. Terleeva, "Oil spills in the Barents Sea based on satellite monitoring using SAR: spatial distribution and main sources," *International Journal of Remote Sensing*, vol. 39, no. 13, pp. 4484–4498, 2017.

[3] M. Mäkynen and M. Similä, "Thin ice detection in the Barents and Kara seas using AMSR2 high-frequency radiometer data," *IEEE Transactions on Geoscience and Remote Sensing*, vol. 57, no. 10, 2019.

[4] A. Doulgeris and A. Cristea, "Incorporating incidence angle variation into SAR image segmentation," *IEEE Int. Geosci. Remote Sens. Symp.*, 2018.

[5] A. Cristea, J. Van Houtte, and A. Doulgeris, "Integrating Incidence Angle Dependencies into the Clustering-Based Segmentation of SAR Images," *IEEE Journal of Selected Topics in Applied Earth Observations and Remote Sensing*, 2020.

[6] M. Mäkynen and J. Karvonen, "Incidence angle dependence of first-year sea ice backscattering coefficient in Sentinel-1 SAR imagery over the Kara Sea," *IEEE Trans. Geosci. Remote Sens*, vol. 55, no. 11, pp. 6170–6181, 2017.

[7] K. Topouzelis and S. Singha, "Incidence angle Normalization of Wide Swath SAR Data for Oceanographic Applications," *Open Geosciences*, vol. 8, no. 1, pp. 450–464, 2016.

[8] W. Lang, P. Zhang, J. Wu, Y. Shen, and X. Yang, "Incidence angle correction of SAR sea ice data based on locally linear mapping," *IEEE Trans. Geosci. Remote Sens*, vol. 54, no. 6, pp. 3188–3199, 2016.